

Preparation, characterization, and properties of new crosslinked proton-conducting membranes with polyoxyalkylene moieties

Ping-Lin Kuo^{a,b,*}, Wu-Jyh Liang^a, Chang-Yu Hsu^b, Wu-Huei Jheng^b

^a Fire Protection and Safety Research Center, National Cheng Kung University, Tainan 70101, Taiwan ROC

^b Department of Chemical Engineering, National Cheng Kung University, Tainan 70101, Taiwan ROC

Received 9 August 2007; received in revised form 3 January 2008; accepted 19 January 2008

Available online 6 February 2008

Abstract

A new class of crosslinked proton-conducting membranes (CPMs) with polyoxyalkylene moieties was designed and prepared based on poly(styrene-*co*-maleic anhydride) modified with 2-aminoethanesulfonic acid sodium salt (AESA-Na) and polyoxyalkylenediamines (PEGDAs). The number density of the pendant of sulfonate group was controlled by the ratio of AESA-Na to PEGDA. The resulted membranes possess good mechanical strength and excellent flexibility. The structural characterizations of these membranes were confirmed by FT-IR and solid-state ¹³C NMR spectra. All these membranes exhibit a wholly amorphous morphology, and show a one-step weight loss from 350 °C, indicating their good thermal stability. The CPM sample with 1.25 mequiv SO₃H per gram reaches the proton conductivity of 0.21 S cm⁻¹ at 30 °C and 0.49 S cm⁻¹ at 95 °C, respectively. Moreover, these protonated membranes show adequate oxidative stability in Fenton's reagent at 30 °C.

© 2008 Elsevier Ltd. All rights reserved.

Keywords: Ionomers; Poly(styrene-*co*-maleic anhydride); Polyoxyalkylene

1. Introduction

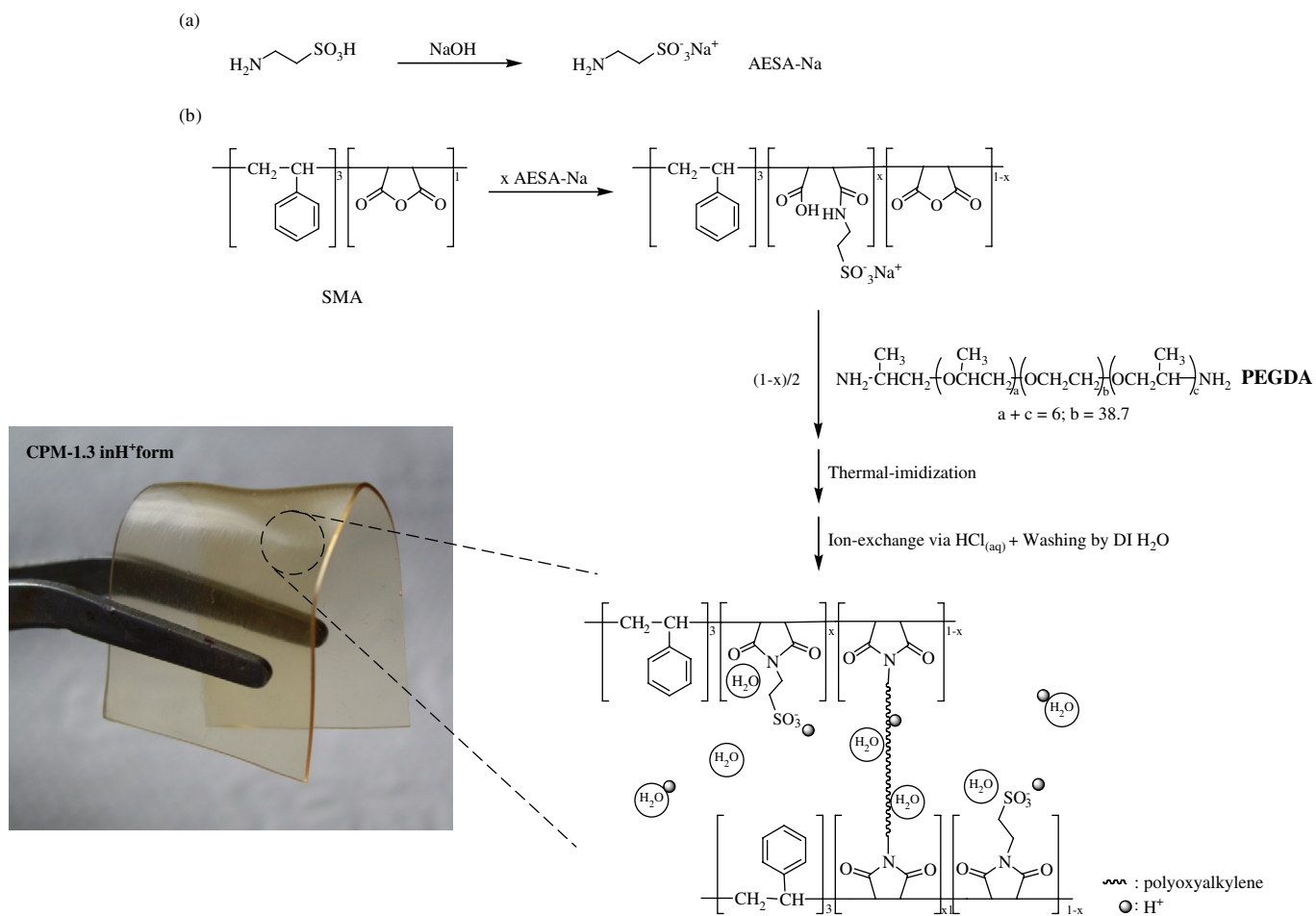
Polymer electrolyte fuel cells (PEFCs) using a proton-conducting ionomer as an electrolyte membrane have been extensively studied for application in electric vehicles, residential power sources, and portable devices [1–3]. The electrolyte membrane acts as a separator to prevent mixing of reactant gases and as a solid ionic conductor to move electrochemically generated protons from the anode to the cathode [4]. Proton conductivity, mechanical strength, and chemical stability of the membrane are major factors that determine fuel cell performance [5]. Much attention continues to be paid to perfluorosulfonate ionomer membranes [6–8], Nafion being the benchmark of proton exchange membrane (PEM), but because of their high cost and

difficulty in synthesis and processing [9–11], efforts are focused on the development of alternatives [12–18].

Functionalization of aromatic polymers with acidic groups is one of the available options for this purpose. Sulfonated poly(ether ether ketone)s (PEEKs) [19], polysulfones (PSFs) [20], poly(arylene ether)s (PAEs) [21], poly(*p*-phenylene)s (PPPs) [22], and phosphoric acid-doped polybenzimidazole (PBI) [23] have been developed for example. Sulfonated polystyrene, in the form of pure polymer, blends, composites and grafted polymer, has also been studied very widely for PEM application [24–27]. Sulfonated polystyrene and its blends have a limitation on the level of sulfonation because the polymer dissolves in water at high levels of sulfonation. Water swelling is a key consideration for proton-conducting polymer electrolyte membranes. Extreme swelling causes a loss of the dimensional stability, while low swelling reduces proton conductivity because of low water absorption of the membranes. Crosslinking is a simple and efficient way to retain indispensable properties such as swelling behavior, dimensional and thermal stabilities [28–31].

* Corresponding author. Fire Protection and Safety Research Center, National Cheng Kung University, Tainan 70101, Taiwan ROC. Tel.: +886 6 275 7575x62658; fax: +886 6 276 2331.

E-mail address: plkuo@mail.ncku.edu.tw (P.-L. Kuo).



Scheme 1. Synthetic route and schematic representation for crosslinked proton-conducting membranes.

To produce a potentially economical and commercially viable polymer electrolyte to meet the requirements for fuel cells, in this study, we have designed and prepared non-fluorinated crosslinked proton-conducting polymers based on poly(styrene-*co*-maleic anhydride) (SMA), 2-aminoethanesulfonic acid sodium salt (AESA-Na) and polyoxyalkylenediamines (PEGDAs). The attached component of AESA-Na through ion-exchanged with H^+ ions acts as proton source, and the other PEGDA having flexible hydrophilic polyoxyalkylene segment is expected to render flexible crosslinking and to percolate proton. FT-IR and ^{13}C solid-state NMR spectroscopies are used to provide information about the microscopic structure and molecular behavior; thermogravimetric analysis (TGA) characterizes the thermal stability; DSC evidences phase transitions in these membranes; complex impedance measurement is used to describe the proton conductivity property. These results are further correlated and discussed.

2. Experimental section

2.1. Materials

Poly(styrene-*co*-maleic anhydride) (SMA, styrene/maleic anhydride = 3:1) was purchased from Elf Atochem.

Polyoxyalkylenediamines (PEGDAs, Jeffamine XTJ-502, Huntsman Corporation) were dehydrated at 80 °C under vacuum for 24 h prior to use. Dimethyl sulfoxide (DMSO, Tedia) was freshly distilled from calcium hydride before use. 2-Aminoethanesulfonic acid (AESA, Sigma), sodium hydroxide (NaOH, Showa), and hydrochloric acid (HCl, RDH) were used as-received. The water used in this study was purified through a Milli-Q Plus system. All other chemicals were of reagent grade and used as-received unless stated otherwise.

2.2. Sample preparation

All crosslinked proton-conducting membranes were synthesized by a simple in situ reaction of SMA, AESA-Na and PEGDA, and the synthetic route is shown in Scheme 1. AESA ion-exchanged with sodium hydroxide at 60 °C for 1 day in the water solution, and 2-aminoethanesulfonic acid sodium salt (AESA-Na) was obtained by evaporating the concentrated solution and drying the solid under vacuum at 85 °C for 1 day. The desired amounts of AESA-Na and SMA were dissolved in appropriate amount of DMSO at 70 °C for 3 h. Subsequently, the stoichiometric amount of PEGDA was added under vigorous stirring at ambient temperature. These solutions were then poured into aluminum plate, and followed

by slowly removing the solvent at 120 °C for 4 h, cured at 150 °C for 24 h. The further thermal imidization reaction of amic acid was proceeded at 200 °C under vacuum for 48 h. All the resulted films were flexible, transparent, and brownish. The thickness of the films was controlled to be in the range of 100–150 μm . Samples are labeled as CPM- x , where x refers to the measured ion-exchange capacity of membranes in mequiv g^{-1} . A typical photograph of CPM-1.3 in H^+ form is shown in Scheme 1. The crosslinked polymer films were also made in the same way without incorporating AESA-Na for comparison, named as CPM-0. Before measuring the membrane performance in terms of proton conductivity, water uptake, and oxidative stability, the membranes in sodium salt form were acidified into protonated form by immersing in 1 N HCl for 2 days, followed by rinsing and washing with deionized water several times.

2.3. Characterizations

2.3.1. FT-IR

FT-IR spectra were measured by using a Nicolet 5700 system with a wavenumber resolution of 2 cm^{-1} , and a minimum of 64 scans were signal-averaged at room temperature. Each sample was prepared by mixing with potassium bromide (KBr) pellet and films were vacuum-dried to remove the absorbed water in the sample.

2.3.2. Solid-state NMR

High-resolution solid-state NMR experiments were carried out on a Bruker AVANCE 400 spectrometer, equipped with a 7 mm double-resonance probe. The Larmor frequencies for ^1H and ^{13}C nuclei are 400.17 and 100.58 MHz, respectively. Magic angle spinning (MAS) of the samples in the range of 3–5 kHz was employed for obtaining NMR spectra. The Hartmann–Hahn condition for $^1\text{H} \rightarrow ^{13}\text{C}$ cross-polarization (CP) experiments was determined using adamantane, and proton decoupling was applied during acquisition to enhance the spectra sensitivity. The ^{13}C and ^1H chemical shifts were externally referenced to tetramethylsilane (TMS) at 0.0 ppm.

2.3.3. Thermal analysis

Thermal analysis of the polymer membranes was performed using both differential scanning calorimetry (DSC, Du Pont TA2010) and thermogravimetric analyzer (TGA, Perkin–Elmer TGA 7). All the measurements were performed under nitrogen. TGA measurements were carried out over a temperature range of 30–800 °C at a heating rate of 20 °C min^{-1} , and the obtained data showing the thermal degradation onset temperature of the samples were used as a reference for DSC measurements. DSC measurements were conducted over the temperature ranges of -150 to 150 °C at a heating rate of 10 °C min^{-1} under dry nitrogen atmosphere. The samples sealed into aluminum pans were first heated at 150 °C for 10 min to remove the thermal history, cooled down to -150 °C and then scanned. The second heating curve was evaluated. All the thermograms are baseline corrected and calibrated against indium metal. Glass transition

temperatures (T_{gs}) were reported as the midpoint of the transition process.

2.3.4. IEC

Ion-exchange capacity (IEC) was measured by titration method. The prepared membranes were soaked in 1 M HCl for 8 h to regenerate the protons from the sodium salt form. They were thoroughly washed with deionized water several times and soaked in 1 M NaCl for 24 h. The protons released due to the exchange reaction with Na^+ ions were titrated against 0.1 M NaOH. The IEC value of membranes was determined from the relationship: $\text{IEC (mequiv g}^{-1}) = V_{\text{NaOH}} \times N_{\text{NaOH}} / \text{weight of polymer}$, where V_{NaOH} is the volume of NaOH consumed and N_{NaOH} is the normality of NaOH.

2.3.5. Water uptake

The crosslinked thin films, after exchange of protons, were dried in a vacuum oven at 100 °C for 24 h. For these thin films, water uptake values were measured by immersing each cross-linked film into water at 30 °C for 24 h. Then the films were taken out, wiped with tissue paper, and quickly weighed on a microbalance. Water uptake (%) of the films was calculated from the equation: $(W_s - W_d) / W_d \times 100$, where W_d and W_s are the weights of dry and corresponding water-swollen film sheets, respectively.

2.3.6. State of water

Two types of water, freezing and nonfreezing water (bound water), in the membranes were detected by melting transitions in DSC measurements as described elsewhere [32–34]. The samples were first cooled from $+25$ to -40 °C with a cooling rate of 5 °C min^{-1} , and then heated at the same rate up to $+25\text{ °C}$. Calculation of the amount of freezing water in the samples was done by integrating the peak area of the melt endotherm. The degree of crystallinity of the water, obtained from the heat of fusion of pure ice (334 J g^{-1}), was used as a standard.

2.3.7. Proton conductivity

Proton conductivity (σ) of the polymer membranes was measured by an ac impedance technique using an electrochemical impedance analyzer (CH Instrument model 604A), where the ac frequency was scanned from 100 kHz to 10 Hz at a voltage amplitude of 10 mV. Fully hydrated membranes were sandwiched into a Teflon conductivity cell equipped with Au plates. The temperature dependence of proton conductivity was carried out by controlling the temperature from 30 to 95 °C at a relative humidity of 95%.

2.3.8. Oxidative stability

A small piece of protonated-membrane sample with a thickness of ca. $150\text{ }\mu\text{m}$ was soaked in Fenton's reagent (30% H_2O_2 containing 30 ppm FeSO_4) at 30 °C . The stability was evaluated by recording the time when the membranes started to break into pieces and dissolved completely.

2.3.9. Tensile strength

The tensile properties of specimens were determined using Instron tensile testing machine equipped with an extensometer. Dumbbell-shaped specimens with a gauge length and a width of 10 and 4 mm, respectively, were stretched with a strain rate of $8.3 \times 10^{-3} \text{ s}^{-1}$ at room temperature. Breaking stress was determined from the stress–strain curve.

3. Results and discussion

3.1. Preparation of the crosslinked SMA-derived membranes with sulfonic acid sodium salt

2-Aminoethanesulfonic acid sodium salt (AESA-Na) was synthesized by the neutralization of aminoethanesulfonic acid and sodium hydroxide, and the structure was confirmed by FT-IR and FAB-MASS spectra. The IR peak at 1050 cm^{-1} corresponded to a vibrational stretching for the salt of sulfonic acid group. The characteristic peaks in the mass spectrum of AESA-Na were well-assigned to the supposed structure.

It is known that the reaction between amino groups and maleic anhydride groups to form an imide structure is feasible and quantitative. In this study, the crosslinked polymer membranes containing ethylsulfonate group were prepared by the conventional two-step procedures as described in Section 2 and as shown in Scheme 1. The degree of thermal conversion of amic acid to imide group was monitored by IR spectroscopy. Each sample was prepared as a thin film, and then treated for measured amounts of time. The degree of imidization was calculated using the following equation [35]:

$$\text{Degree of imidization} = \frac{[A_1/A_2]_t - [A_1/A_2]_{t=0}}{[A_1/A_2]_{t=\infty} - [A_1/A_2]_{t=0}}$$

where A_1 is the absorbance of imide peak at 1775 cm^{-1} , A_2 is the absorbance of standard reference peak at 1490 cm^{-1} , and $t = \infty$ is taken as the time beyond which no further changes in the imide peak was observed at 200°C . No imidization was observed in the polymer films before heating. When the sample was heated, the imide peak gradually grew and remained invariant. The quantitative IR analysis of percent imidization for the prepared membranes with sulfonic acid sodium salt is tabulated in Table 1. All flexible and transparent films were obtained after thermal cyclodehydration (imidization).

Table 1
Structural data for CPM samples in Na^+ form

Polymer code	AESA-Na/PEGDA (mol/mol)	Imidization ^a (%)	IEC ^b (mequiv g^{-1})
CPM-1.3	8.0	92	1.25
CPM-1.0	5.3	90	0.96
CPM-0.8	3.2	95	0.77
CPM-0.5	1.5	91	0.47
CPM-0.3	0.6	100	0.29

^a Determined from FT-IR.

^b Evaluated by titration.

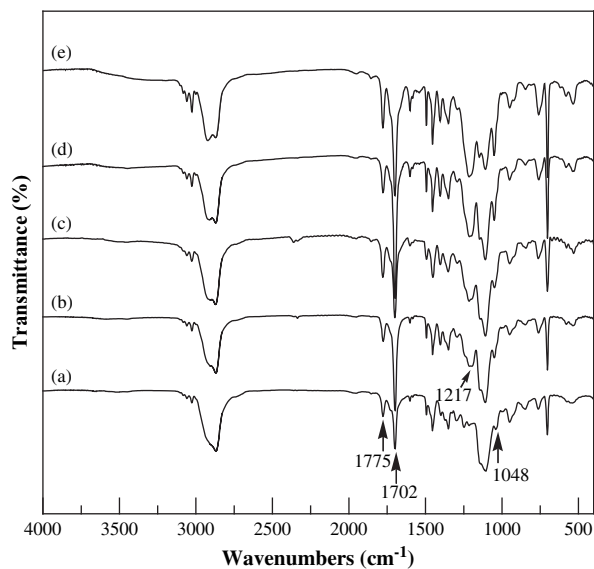


Fig. 1. FT-IR spectra of CPM- x in Na^+ form: $x =$ (a) 0.3; (b) 0.5; (c) 0.8; (d) 1.0; (e) 1.3.

3.2. FT-IR

To confirm the chemical structure of the prepared crosslinked membranes in Na^+ form, FT-IR spectra were collected and shown in Fig. 1. As shown in Fig. 1, the characteristic absorption bands of imide carbonyl group at around 1702 (symmetric) and 1775 cm^{-1} (asymmetric) confirm the formation of imide rings. Two peaks at 1048 and 1217 cm^{-1} evidencing the S–O stretching typical of the sulfonate groups are clearly observed [36,37], and the intensity increases with the amount of the incorporated sulfonate group. The C–N–C absorption of the imide ring is observed at around 1342 cm^{-1} . These results show that all the ethylsulfonate group containing membranes were successfully prepared, and the absence of the absorption bands of valence oscillation of cyclic anhydride structure of SMA at 1780 and 1857 cm^{-1} in all samples indicates the completion of crosslinking.

Furthermore, as shown in Fig. 1, it is observed that the changes in frequencies and shape of the C–O–C stretching mode (ca. 1100 cm^{-1}) with the increasing $-\text{SO}_3^- \text{Na}^+$ concentration are associated with different micro-arrangement. Probably, the basic ether oxygens of polyether chains interact with acceptor groups to a greater extent in these polymer networks, and are correlated to the sodium cation coordination. Similar behavior has been observed in lithium-ion conducting polymers [38,39].

3.3. ^{13}C CP/MAS NMR

Solid-state ^{13}C CP/MAS NMR spectra were also introduced to investigate the structure of the crosslinked polymer membranes in Na^+ form. Fig. 2 shows the ^{13}C CP/MAS NMR spectra of the prepared samples with different sulfonate contents, together with the assignments of the peaks. As shown in Fig. 2, one peak at ca. 17 ppm is due to the methyl groups

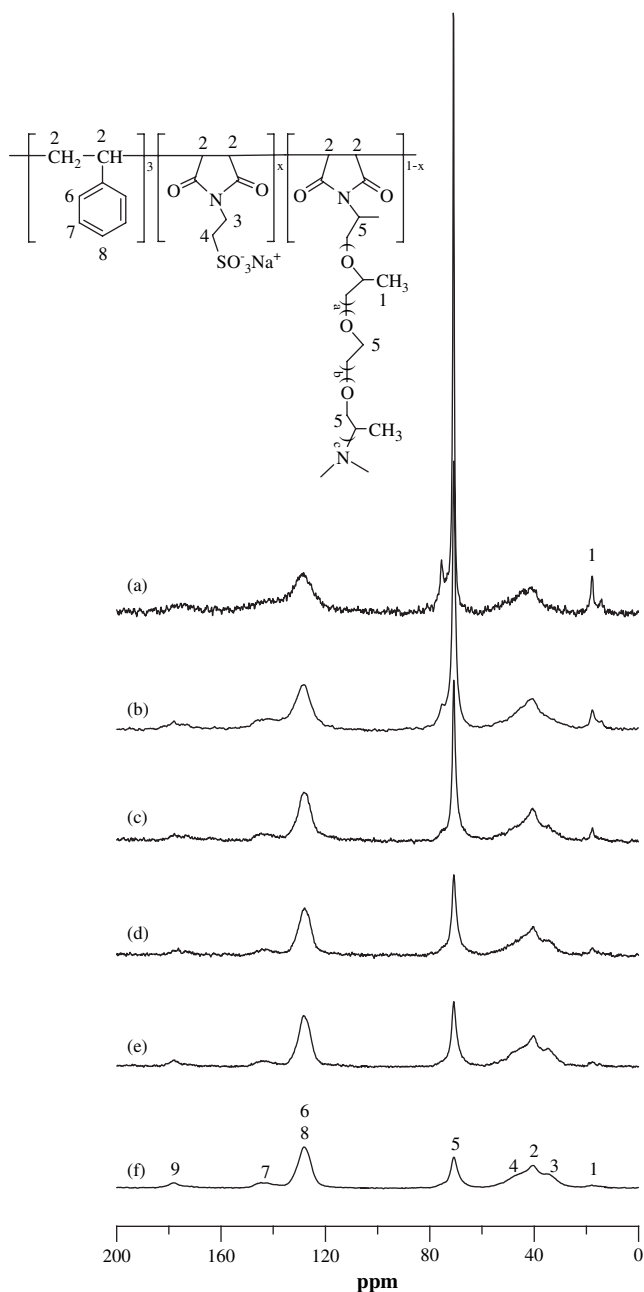


Fig. 2. ^{13}C CP/MAS NMR spectra of CPM- x in Na^+ form, together with the assignments of the peaks: $x =$ (a) 0; (b) 0.3; (c) 0.5; (d) 0.8; (e) 1.0; (f) 1.3.

on the PPO backbone. The overlapped signal located at around 40 ppm is attributed to the methylene groups of backbone. Two peaks at 33 and 48 ppm are assigned to the methylene carbons in β - and α -position to the sulfonate group, respectively. Besides, the resonance peaks at ca. 70 ppm are associated with the polyether backbone moieties. The peaks at 128 and 143 ppm are attributed to the *ortho*- and *para*-position and the *meta*-position carbons on phenyl ring, respectively. The peak at 177 ppm corresponds to those carbonyl carbons of backbone.

From Fig. 2, it is observed that as the content of sulfonate group increases, the intensity of the peak at 128 ppm is normalized; the intensity of the peaks corresponding to the sulfonate group increases and that of the peak due to polyether

moieties decreases. Also, the line broadening and the displacement to lower ppm values are observed with the peak of the methylene carbons in polyether block. This indicates that the presence of sulfonic acid sodium salt causes a more broad distribution of the polyether-segment environments and/or reduces the segmental motion of the polymer chains; the latter results from the electronic interaction between the Na^+ cations and the ether oxygens in polyether segments.

3.4. IEC

Ion-exchange capacity (IEC) provides an indication of the ion-exchangeable groups present in a polymer matrix, which are responsible for the conduction of protons and thus is an indirect and reliable approximation of the proton conductivity. For this reason, high IEC value is desired for proton-conducting membranes. However, with the increase in the content of sulfonic acid group, the polymer becomes more hydrophilic and the stability towards water and other mechanical properties will be decreased [40]. Hence, it is very essential to optimize the amount of sulfonic acid group, which can be accomplished, in this study, by controlling the ratio of AESA- Na and PEGDA. The measured IEC values of the prepared membranes in this study are listed in Table 1. It can be seen in Table 1 that the IEC values of these crosslinked membranes increase with increasing AESA- Na content, and are in the range of 0.29–1.25 mequiv g^{-1} .

3.5. Thermal behavior

The synthesized crosslinked membranes, CPM- x , in Na^+ form were subjected to DSC/TGA measurements to evaluate their thermal transition and decomposition properties. The samples were dried in a vacuum oven overnight at 120 $^{\circ}\text{C}$ prior to measurements. Fig. 3 shows the TG curves measured under flowing nitrogen for all the prepared samples. As shown in Fig. 3, all the TG curves are very similar (except for the

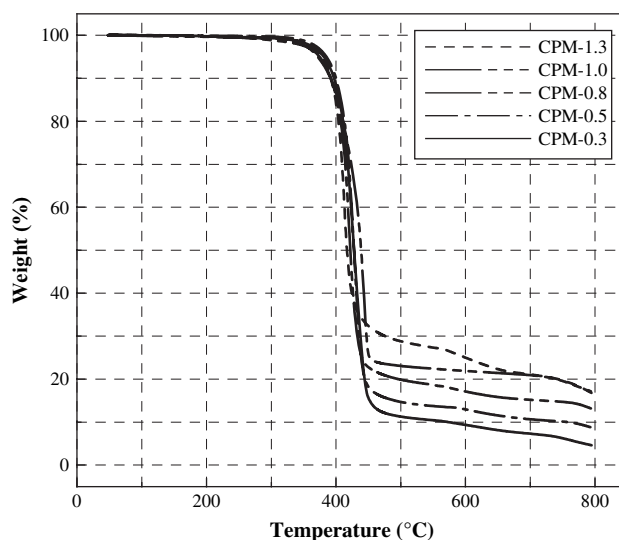


Fig. 3. TGA thermograms of CPM- x in Na^+ form under nitrogen atmosphere.

amount of residue) among CPM-*x* membranes in Na⁺ form with different composition; one-step weight loss from 350 °C is observed, which is higher than that of other miscellaneous polyimide electrolytes that started to decompose by the cleavage of C_{Ar}-SO₃⁻ bonds at ca. 280 °C [41,42]. With further introduction of ethylsulfonate, ethylsulfonate oxidation of polyether phase can cause the thermal event at ~500 °C, and the amount of residue of polymer membranes increases.

Fig. 4 shows the DSC thermograms of chemically cross-linked CPM-*x* in Na⁺ form with different binary crosslinking compositions of AESA-Na and PEGDA. As shown in Fig. 4, the sample without incorporating AESA-Na (CPM-0) shows two second-order transitions at very different temperatures. The lower transition temperature (T_{g1}) at around -48 °C is attributed predominantly to the motion of the flexible polyether segments of the network, and the small inflection centered at around 53 °C (T_{g2}) corresponds to the glass transition temperature of the network above which the chain motion takes place. Changing the binary crosslinking compositions leads to the thermal events change. In comparison with the CPM-0 sample, an observable change in T_{g1} with increasing -SO₃⁻Na⁺ concentration is noticed, for example from -48 °C for CPM-0 to -38 °C for CPM-0.5, and a further increase to -24 °C for CPM-1.3. This shift in T_{g1} can be attributed to the ionic crosslinking occurring between the cation and the ether oxygens. The change in T_{g2} could be as a result of the mutual influences on the behaviors of grafting, crosslinking, and ion-dipole interactions. In addition, as shown in Fig. 4, no melting transition exists for any of the samples in the range of analyzed temperature, indicating no existence of crystalline structure in polymer networks. The amorphous nature in these crosslinked electrolytic membranes is favorable for high water uptake because water molecules can easily diffuse into the amorphous region with looser molecular packing.

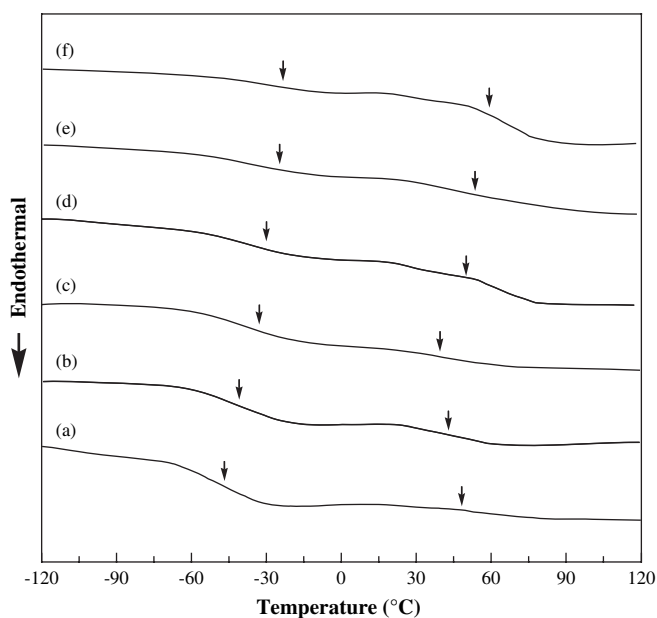


Fig. 4. DSC curves of CPM-*x* in Na⁺ form: *x* = (a) 0; (b) 0.3; (c) 0.5; (d) 0.8; (e) 1.0; (f) 1.3.

Table 2
Properties of fully hydrated CPM and Nafion 117 at 30 °C

Sample ^a	Water uptake (%)	Bond water ^b (%)	Specific H ⁺ concentration (mequiv g ⁻¹)	$\sigma \times 10^2$ (S cm ⁻¹)	Breaking stress $\times 10^{-2}$ (Pa)
CPM-1.3	230	14	0.38	20.8	6.9
CPM-1.0	199	20	0.32	19.5	9.2
CPM-0.8	163	25	0.29	15.9	13.2
CPM-0.5	139	33	0.20	2.8	14.4
CPM-0.3	134	36	0.12	2.1	35.0
Nafion 117	19	14	0.77	3.1	219.5

^a As H⁺ form.

^b Obtained by DSC.

3.6. Water uptake and state of water

Following the exchange of Na⁺ with H⁺, membranes were equilibrated in deionized water, and their water uptake was determined and listed in Table 2. From Table 2, it can be found that all the prepared samples reach high water uptake, in excess of 130%. The water sorption strongly depends on the content of sulfonic acid groups in the network matrix; the higher the content of sulfonic acid groups, the larger the water uptake. Larger sorption of water may be caused by the greater hydrophilicity of the polymer segments or the flexibility/microstructure of the polymer networks.

Water sorption characteristics are of great importance for proton-conducting polymer membranes. The state of water such as free water and bound water in sulfonated polymers directly affect the transportation of proton across the membranes. The DSC thermograms of the fully hydrated CPM-*x* membranes in H⁺ form in Fig. 5 show that all the samples have an endothermic peak at around -10 to 5 °C. The membranes with higher IEC clearly show a higher melting point. The association of water molecules with other species such

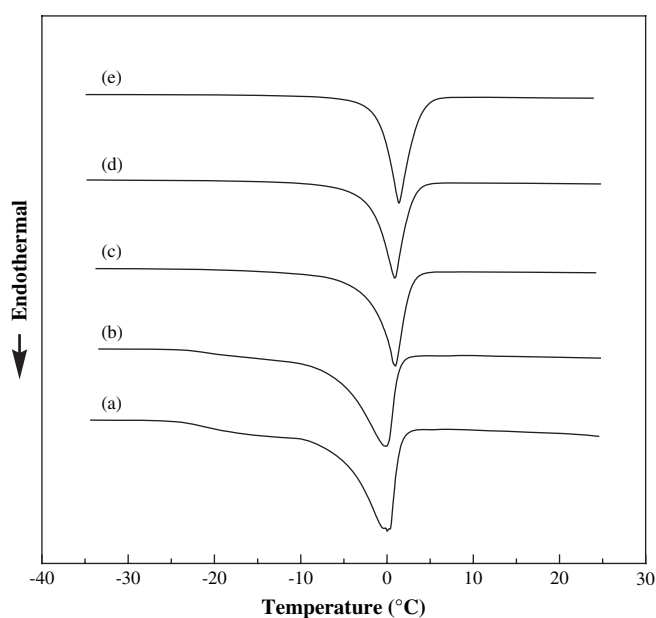


Fig. 5. DSC thermograms indicating the melting of water in the fully hydrated CPM-*x* in H⁺ form: *x* = (a) 0.3; (b) 0.5; (c) 0.8; (d) 1.0; (e) 1.3.

as ionic and polar groups dominates the thermal transitions of water molecules. It has been shown that the bound water that forms a true solution with the polymer does not freeze at 0 °C and the melting endotherm observed in a DSC thermogram at that temperature is due to the free and loosely bound water. The weight fraction of free water to the fully hydrated membranes can be estimated from the total melting enthalpy (ΔH_m) that is obtained by integration of the transition heat capacity over the broad melting temperature interval.

$$\text{Free water}(\%) = \frac{\Delta H_m}{334(\text{J g}^{-1})}$$

The weight fraction of bound water is calculated by subtracting the amount of freezing water from the total mass fraction of water in the membranes. As can be seen in Fig. 5 and Table 2, the decreasing melting point with increasing polyoxyalkylene concentration in these membranes can be attributed to the increasing percentage of bound water.

3.7. Proton conductivity measurements

The temperature dependencies of proton conductivity (σ) at constant relative humidity (RH) of 95% for CPM- x membranes in H^+ form are shown in Fig. 6. Factors that determine proton conductivity are the concentration and mobility of the charge carriers in the membrane. From Fig. 6, the proton conductivity increases with increasing content of sulfonic acid groups, and the temperature dependence is changed from a curvature relation to more linear-like one. In addition, the apparent activation energy for proton conduction, which is obtained from the slope of the plot, decreases with an increase in the content of sulfonic acid. These suggest that the proton conduction mechanism appears to change, and the proton transport

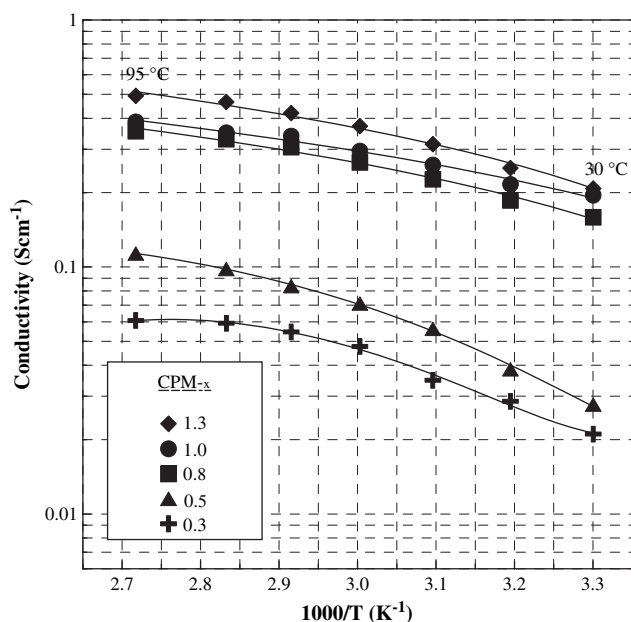


Fig. 6. Temperature dependence of the proton conductivity for CPM- x membranes in H^+ form.

becomes less coupled with the segmental motions of polymer chains as the content of sulfonic acid is increased. That is, for the CPM-0.3 and CPM-0.5 samples, a Grotthus-type mechanism dominates the ionic conduction, whereas a vehicle-type mechanism appears to be the primary route of conduction for the samples with $x > 0.5$ [43].

Additionally, as the sulfonic acid content increases, the changes in free volume, electrostatic interactions, and hydrogen-bonding interaction will affect proton conduction. The increase in proton conductivity with the sulfonic acid content may be due to the increased number of the charge carriers and the increased water uptake in the membrane, as shown in Table 2. From Table 2, the specific H^+ concentration indicates the equivalent amount of proton in swollen membranes. The presence of water in the membrane would act as the active site of the proton transport via hydrogen bonding, and also makes the polymeric chain flexible, and consequently the carrier ions are easy to transport in membrane. Furthermore, the proton conduction would proceed through the molecular coordination of proton with ethylene oxide units in the host matrix [44].

When temperature is raised, molecular diffusion results in fast proton conduction, and meantime the dimensional change of these swollen membranes is obviously observed due to the loss of absorbed water. Nevertheless, these crosslinked membranes still retain good apparently mechanical strength. The crosslinked membrane with IEC of $1.25 \text{ mequiv g}^{-1}$ under 95% RH exhibits the proton conductivity of 0.21 S cm^{-1} at 30 °C and 0.49 S cm^{-1} at 95 °C, respectively.

3.8. Oxidative stability

Oxidative stability of the protonated membranes (ca. $150 \mu\text{m}$) was evaluated by observing the dissolving behavior in Fenton's reagent at 30 °C, and the results are tabulated in Table 3. Obviously, both τ_1 and τ_2 become shorter by the increase in the ethylsulfonate group content due to its higher water-absorbing capability as shown in Table 2. Since the oxidative species such as HO^\bullet and HOO^\bullet accompany some water molecules when reacting to the substrates. Interestingly, it is noticed that all the membranes of CPM- x in this study show better oxidative stability than that of an electrolyte membrane based on arylene ether/fluorinated alkane copolymer [45]. The

Table 3
Oxidative stability of CPM and Nafion 117 at 30 °C in Fenton's reagent

Sample ^a	τ_1^b (h)	τ_2^b (h)
CPM-1.3	7	11
CPM-1.0	8	13
CPM-0.8	12	15
CPM-0.5	20	25
CPM-0.3	>48	>48
Nafion 117	>48	>48
Fluorinated arylene copolymers ^c	4	6

^a As H^+ form.

^b τ_1 and τ_2 refer to the expended time that the membranes became a little brittle and started to dissolve in the solution, respectively.

^c From Ref. [45].

CPM-1.3 membrane endured for 11 h before it started to dissolve.

3.9. Tensile strength

In this study, the breaking stress of the fully hydrated CPM in H⁺ form is determined from the stress–strain curve measured at a strain rate of $8.3 \times 10^{-3} \text{ s}^{-1}$, and the obtained results are tabulated in Table 2. Each value was obtained from the average of five individual tensile tests. From Table 2, it is evident that the breaking stress is dependent on the ratio of AESA-Na and PEGDA, and is reduced as the content of sulfonic acid is increased. This can be related to the lower cross-linking density and the higher water uptake of the membrane. The value of breaking stress is decreased from 35 to $6.9 \times 10^2 \text{ Pa}$, correspondingly. Also, the value of Nafion 117 is shown as a comparison.

4. Conclusions

We have successfully developed a new class of crosslinked proton-conducting membranes based on SMA modified with AESA-Na and further crosslinked with PEGDA. The prepared membranes exhibit promising swelling characteristics, a good mechanical strength, and flexibility. All the membranes are thermally stable and do not decompose up to ca. 350 °C. In this study, the membrane with IEC of 1.25 mequiv g⁻¹ under 95% RH exhibits the proton conductivity of 0.21 S cm⁻¹ at 30 °C and 0.49 S cm⁻¹ at 95 °C, respectively. It has the potential for technological application in polymer electrolyte fuel cells.

Acknowledgements

The authors would like to thank the National Science Council, Taipei, Taiwan ROC for their generous financial support of this research.

References

- [1] Lemmons RJ. *J Power Sources* 1990;29:251.
- [2] Strasser K. *J Power Sources* 1992;37:209.
- [3] Kordesch K, Simander G, editors. *Fuel cells and their applications*. Weinheim: Wiley-VCH; 1996.
- [4] Appleby AJ, Foulkes RL, editors. *Fuel cell handbook*. New York: Van Nostrand; 1989.
- [5] Niedrach LW, Grubb WT, editors. *Fuel cells*. New York: Academic Press; 1963. p. 259.
- [6] Zawodzinski TA, Springer TE, Uribe F, Gottesfeld S. *Solid State Ionics* 1993;60:199.
- [7] Savadogo O. *J New Mater Electrochem Syst* 1998;1:47.
- [8] Slade S, Campbell SA, Ralph TR, Walsh FC. *J Electrochem Soc* 2002; 149:A1556.
- [9] Sumner JJ, Creager SE, Ma JJA, Desmarteau DD. *J Electrochem Soc* 1998;145:107.
- [10] Samms PS, Wasmus S, Savinell RF. *J Electrochem Soc* 1996;26:909.
- [11] Jia N, Lefebvre MC, Halfyard J, Qi Z, Pickup PG. *Electrochem Solid State Lett* 2000;3:529.
- [12] Hickner MA, Ghassemi H, Kim YS, Einsla BR, McGrath JE. *Chem Rev* 2004;104:4587.
- [13] Schuster MFH, Meyer WH. *Annu Rev Mater Res* 2003;33:233.
- [14] Roziere J, Jones DJ. *Annu Rev Mater Res* 2003;33:503.
- [15] Rikukawa M, Sanui K. *Prog Polym Sci* 2000;25:1463.
- [16] Yang Y, Shi Z, Holdcroft S. *Macromolecules* 2004;37:1678.
- [17] Norsten TB, Guiver MD, Murphy J, Astill T, Navessin T, Holdcroft S, et al. *Adv Funct Mater* 2006;16:1814.
- [18] Qiao J, Hamaya T, Okada T. *Chem Mater* 2005;17:2413.
- [19] Jones DJ, Roziere J. *J Membr Sci* 2001;185:41.
- [20] Wang F, Hickner M, Ji Q, Harrison W, Mecham J, Zawodzinski TA, et al. *Macromol Symp* 2001;175:387.
- [21] (a) Cabbaso I, Yuan Y, Mittelsteadt C. US Patent 5989742; 1999; (b) Miyatake K, Chikashige Y, Watanabe M. *Macromolecules* 2003;36: 9691.
- [22] Kobayashi T, Rikukawa M, Sanui K, Ogata N. *Solid State Ionics* 1998; 106:219.
- [23] Wainright JS, Wang JT, Weng D, Savinell RF, Litt M. *J Electrochem Soc* 1995;142:L121.
- [24] Carretta N, Tricoli V, Picchioni F. *J Membr Sci* 2000;166:189.
- [25] Ding J, Chuy C, Holdcroft S. *Macromolecules* 2002;35:1348.
- [26] Chen N, Hong L. *Polymer* 2004;45:2403.
- [27] Bae B, Kim D. *J Membr Sci* 2003;220:75.
- [28] Depre L, Ingram M, Poinsignon C, Popall M. *Electrochim Acta* 2000;45: 1377.
- [29] Kerres JA. *J Membr Sci* 2001;185:3.
- [30] Mikhailenko SD, Wang K, Kaliaguine S, Xing P, Robertson GP, Guiver MD. *J Membr Sci* 2004;233:93.
- [31] Kerres JA. *Fuel Cells* 2005;5:230.
- [32] Karlsson LE, Wesslen B, Jannasch P. *Electrochim Acta* 2002;47:3269.
- [33] Nakamura K, Hatakeyama T, Hatakeyama H. *Polymer* 1983;24:871.
- [34] Ostrovskii DI, Torell LM, Paronen M, Hietala S, Sundholm F. *Solid State Ionics* 1997;97:315.
- [35] Rao CNR, editor. *Chemical applications to infrared spectroscopy*. New York: Academic; 1963. p. 534–6.
- [36] Erdemi H, Bozkurt A, Meyer WH. *Synth Met* 2004;143:133.
- [37] Ding J, Chuy C, Holdcroft S. *Chem Mater* 2001;7:2231.
- [38] Kuo PL, Liang WJ, Chen TY. *Polymer* 2003;44:2957.
- [39] Liang WJ, Chen YP, Wu CP, Kuo PL. *J Phys Chem B* 2005;109:24311.
- [40] Genies C, Mercier R, Sillion B, Cornet N, Gebel G, Pineri M. *Polymer* 2001;42:359.
- [41] Miyatake K, Zhou H, Watanabe M. *Macromolecules* 2004;37:4956.
- [42] Lee C, Iyer S, Kwon J, Han H. *J Polym Sci Part A Polym Chem* 2004; 42:3621.
- [43] Zukowska G, Chojnacka N, Wieczorek W. *Chem Mater* 2000;12:3578.
- [44] Qiao J, Yoshimoto N, Ishikawa M, Morita M. *Chem Mater* 2003;15: 2005.
- [45] Miyatake K, Oyaizu K, Tsuchida E, Hay AS. *Macromolecules* 2001;34: 2065.